14TH CANADIAN MASONRY SYMPOSIUM
MONTREAL, CANADA
MAY 16TH – MAY 20TH, 2021

STATIC-CYCLIC TESTS ON MASONRY WALL WITH ASYMMETRIC OPENING

Kovarbašić, Milan[1]; Salzmann, Roman[2] and Mojsilović, Nebojša [3]

ABSTRACT

Past earthquakes show that unreinforced masonry (URM) walls with door or window openings are among the most vulnerable structures to fail in-plane. In order to improve the understanding of their load-deformation behavior, two static-cyclic shear tests were performed on a storey-high URM wall with an asymmetric door opening and a shear-span ratio that represents an internal wall in a two-storey building. The wall was constructed using standard perforated Swiss clay blocks and standard cement mortar. The experimental results showed asymmetric response of the wall specimen due to the eccentric door opening. After reaching a certain drift ratio, local increase of normal stresses in the narrower wall pier, next to the door opening, had a detrimental impact on the propagation of diagonal shear cracks resulting in a brittle failure and limited displacement capacity of the wall. Wall geometry and shear-span ratio exhibited a significant impact on the load-deformation behavior of the URM wall with a door opening. Furthermore, an empirical model based on Swiss Structural Masonry Code recommendations was used to estimate the deformation capacity of the wall specimen with the boundary conditions applied in the test. This paper presents and discusses the results obtained from the abovementioned experiments as well as from the code empirical prediction.

KEYWORDS: *asymmetric wall opening, displacement capacity, shear-span ratio, static-cyclic shear, unreinforced masonry*

[1]PhD Student, Institute of Structural Engineering, ETH Zurich, Switzerland, kovarbasic@ibk.baug.ethz.ch
[2]Dr Lüchinger+Meyer Bauingeniuere AG, Zurich, Switzerland, rsa@luechingermeyer.ch
[3]Senior Scientist, Institute of Structural Engineering, ETH Zurich, Switzerland, mojsilovic@ibk.baug.ethz.ch

INTRODUCTION

Due to their quasi-brittle behaviour, URM structures perform poorly in earthquakes. Seismic assessment of typical URM buildings takes into consideration in-plane as well as out-of-plane actions. The risk of out-of-plane wall failures can be minimized with proper connections between walls and floor diaphragms. On the other side, the seismic capacity of such buildings might depend on the strength and ductility of walls loaded in-plane. Past earthquakes [1] showed greater vulnerability due to seismic events of in-plane loaded URM walls with openings compared to solid URM walls. Previous tests were mainly focused on wall piers only and scarcely on spandrels [2]. Some experimental programs [3] [4] [5] have been conducted on perforated URM walls to better understand their global response under lateral loading. However, these tests were performed on wall specimens with symmetric openings, even though architectural design requires openings to be most often placed eccentrically. Recent tests on URM walls with arched openings [6] showed that asymmetric openings have an impact on lateral load capacities and failure modes.

The aim of the tests reported in this paper is to contribute to the understanding of the in-plane force-displacement capacity and failure modes of URM walls with rectangular door openings. The focus was to investigate the influence of asymmetric opening and shear-span ratio for walls within two-storey buildings.

GEOMETRICAL AND MATERIAL WALL PROPERTIES

The tested wall feature the rectangular shape with the length of 2.7 m, the height of 2.6 m and the wall thickness of 150 mm. The wall has an asymmetric door opening of 0.9 x 1.9 m with a standard, prefabricated masonry lintel. Typical Swiss perforated clay blocks with nominal dimensions of 290/150/190 mm, and standard cement mortar were used to construct the specimen. The specimen was built by professional bricklayers. The blocks were tested according to EN 772-1 [7] on a sample of 10 blocks. Characterization of standard cement mortar was done according to EN 1015 [8] by testing mortar prisms 40/40/160 mm. Two sets of samples, one stored in a climate room and the other in ambient conditions, were tested after a storage time of 62 days. The masonry compressive strength and modulus of elasticity were determined in accordance with EN 1052-1 [9] on specimens with nominal dimensions of 1000/600/150 mm. Summary of determined material properties is given in Table 1.

Table 1: Summary of masonry material properties

Material	Compressive strength [MPa]	Bending strength [MPa]	Modulus of elasticity [GPa]
Brick	24.1	-	-
Mortar (climate room)	14.9	4.63	-
Mortar (ambient)	2.77	1.06	-
Masonry	5.14	-	4.21

TEST SETUP, TEST PROGRAMME AND INSTRUMENTATION

The tests were conducted in the three-actuator setup shown in Figure 1. The specimen (1) was constructed on the 450 mm high reinforced concrete (RC) pedestal (2), which was clamped to the strong floor (3) using post-tensioning steel rods. Lateral displacements were applied at the top of the wall by means of the horizontal servo-hydraulic actuator (4) connected to the reaction wall (5). Vertical forces and moments at the wall top were controled using two-servo hydraulic actuators (8) connected to the reaction frame (9). A stiff horizontal steel loading beam (6) served as the interface between three servo-hydraulic actuators and the specimen. Uniform displacement and load transfers were ensured by 10 mm thick mortar layer (7) between the steel loading beam and the wall top.

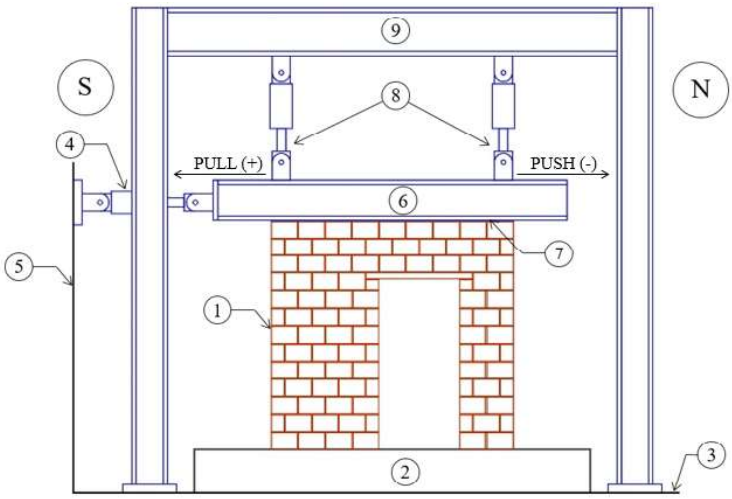

Figure 1: Three-actuator setup

In the first step, two vertical servo-hydraulic actuators, south and north, imposed compressive loads of $V_{S0} = V_{N0} = -68.3$ kN using linear force ramps while the horizontal force was set to zero. Together with the weight of horizontal steel loading beam of 26 kN and the wall self-weight, the applied axial stress corresponds to approximately 10% of the masonry compressive strength. Subsequently, the specimen was subjected to lateral displacements in the form of saw tooth cycles. The tests started with a pull semi-cycle (positive values of shear force and displacement). Each cycle was repeated three times with a displacement speed of 0.1 mm/s. Simultaneously, two vertical servo-hydraulic actuators were used to apply bending moments at the top of the wall in force control. Two loading histories were created such that they are equivalent in terms of target displacements and boundary conditions to hybrid tests conducted on the wall with the same geometrical and material properties. More information about the substructuring scheme of the prototype two-storey internal wall, selected ground motions and results of hybrid tests can be found in Miraglia et al. (2020) [10]. The target displacements in these two loading histories represent the serviceability limit state (SLS) and the ultimate limit state (ULS) of the tested masonry wall. Therefore, testing phases in the paper are further defined as the SLS and the ULS tests. Bending moments at the wall top were obtained based on force differences measured in vertical servo-

hydraulic actuators during hybrid tests. Force differences in vertical servo-hydraulic actuators were related to horizontal displacements applied at the wall top. In each step, vertical forces are corrected based on the horizontal displacement command (d_H) multiplied by factor m which was obtained by means of linear regression, see Figure 2. Total vertical forces remained unchanged. The forces applied in the servo-hydraulic actuators south and north are described by equations (1) and (2) respectively. Loading histories applied in the SLS and the ULS test are given in Figure 3. Note the different axis scales for SLS and ULS tests in Figures 2 and 3. The same is also true for the Figures 5, 8, 9 and 10 on the following pages.

$$V_S = V_{S0} - m \cdot d_H \tag{1}$$

$$V_N = V_{N0} + m \cdot d_H \tag{2}$$

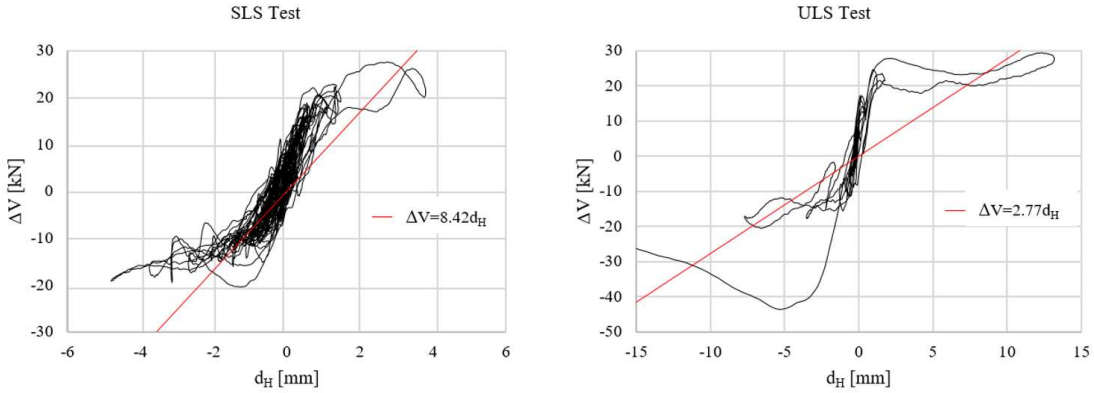

Figure 2: Force differences in vertical servo-hydraulic actuators for displacements at the wall top and determined linear relationships for SLS test (left) and ULS test (right)

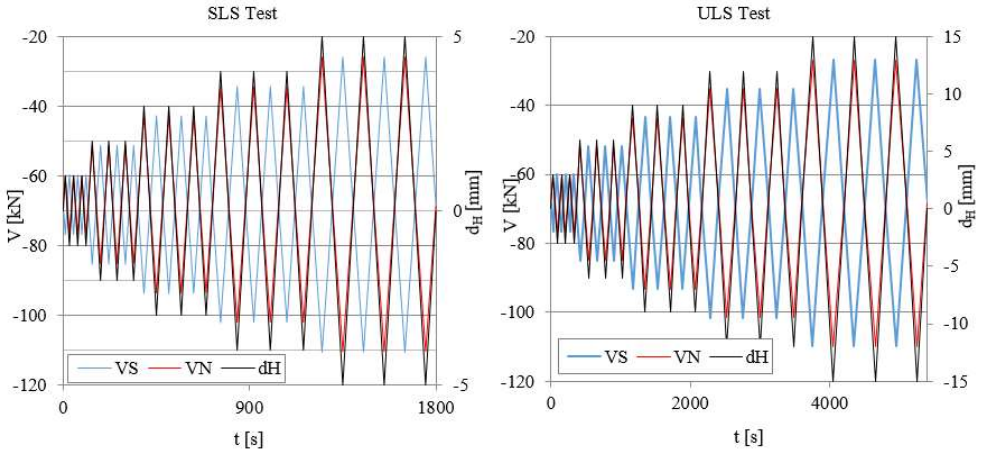

Figure 3: Loading histories: SLS test (left) and ULS test (right)

A three-channel INOVA system controled the servo-hydraulic actuators. An INDEL GIN-SAM4 real-time computer was connected to the INOVA control system via EtherCAT and used to send

displacement and force commands. Moreover, the INDEL GIN-SAM4 real-time computer was used to collect external linear variable differential transformers (LVDTs) measurement data and to trigger the digital image correlation (DIC) system at the pre-defined displacements in each cycle applied. LVDTs were mounted in such a way to measure masonry deformations, relative sliding and uplifting of the wall to the reaction frame and the RC pedestal at multiple postitions. The 2D-DIC system was used to obtain the in-plane displacement field of the wall surface. For that purpose, a random speckle pattern with dot size of approximately 1.5 mm was applied on the wall surface. More information about the implemented DIC system can be found in Mojsilovic and Salmanpour [11]. The LVDTs instrumentation plan and the DIC installation are shown in Figure 4.

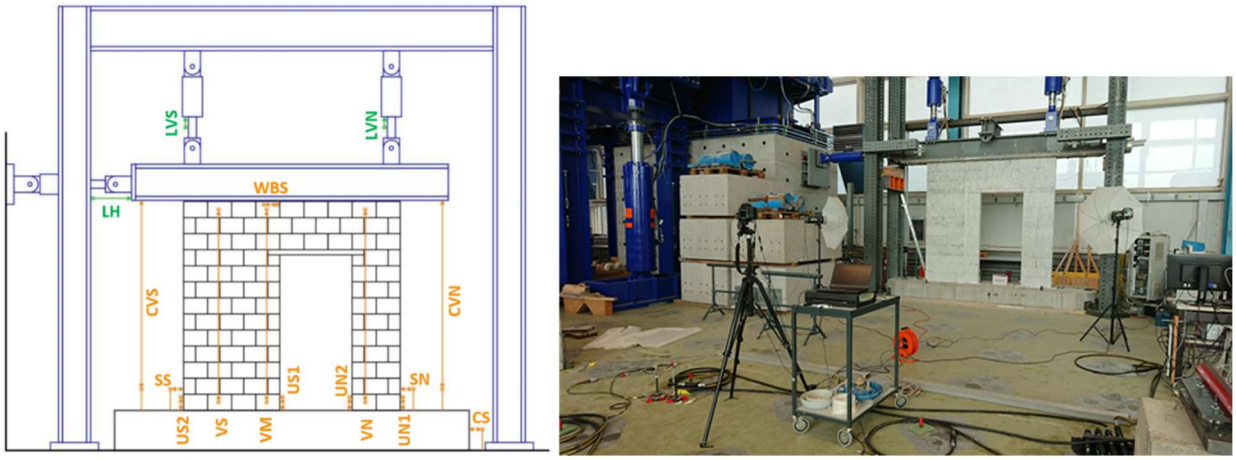

Figure 4: LVDTs instrumentation layout (left) and DIC installation (right)

TEST RESULTS

The values of extreme horizontal forces, H_{push} and H_{pull}, and horizontal displacements, d_{push} and d_{pull}, during "push" (negative values) and "pull" (positive values) semi-cycles recorded in the SLS and the ULS tests are summarized in Table 2. Furthermore, the extreme horizontal displacements in terms of drift ratio, δ_{push} and δ_{pull} are also given. The horizontal force-displacement response hysteresis curves of the SLS and the ULS tests are presented in Figure 5.

Table 2: Measured response extreme values

Test	H_{push} [kN]	H_{pull} [kN]	d_{push} [mm]	d_{pull} [mm]	δ_{push} [%]	δ_{pull} [%]
SLS	-32.5	47.4	-5	5	-0.19	0.19
ULS	-40.6	56.5	-12	12	-0.46	0.46

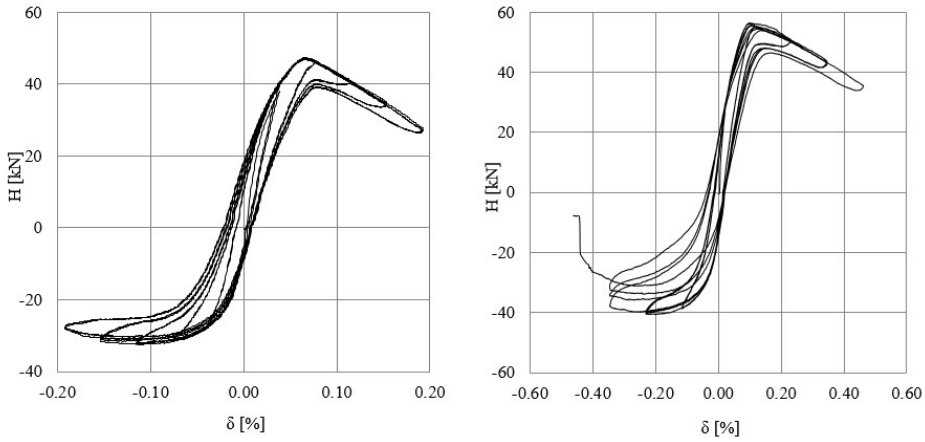

Figure 5: Horizontal force-displacement response hysteresis curves: SLS test (left) and ULS test (right)

SLS Test

The wall showed an asymmetric response due to the eccentric door opening. The maximum horizontal force of pulling semi-cycles was higher in comparison to the maximum horizontal force of pushing semi-cycles. The application of displacements on the specimen in the pulling direction resulted in the formation of horizontal cracks through the mortar joints on both wall piers, left and right from the door opening. During the second load cycles with a target displacement of 2 mm (corresponding to a horizontal drift ratio of 0.08%) a clearly visible horizontal crack along the mortar joint in the upper part of narrower wall pier opened. After reaching the horizontal force peak with the horizontal drift ratio of 0.07%, the stiffness of the wall started to drop rapidly and the wall developed predominantly rocking response during pulling semi-cycles. On the other hand, only small reduction of the horizontal force was observed while the wall was pushed. When applying pushing displacements, a single horizontal crack occurred in the mortar layer between the first and the second brick layer in the wider wall segment. In addition, a staircase-like crack starting at the upper left corner of the door-opening was formed and continuously grew with applied lateral displacements. Figure 6 shows crack patterns in the wall mapped by plotting the von Mises strain fields obtained from the DIC analysis for target displacements of +/- 5 mm (horizontal drift ratio of 0.19%).

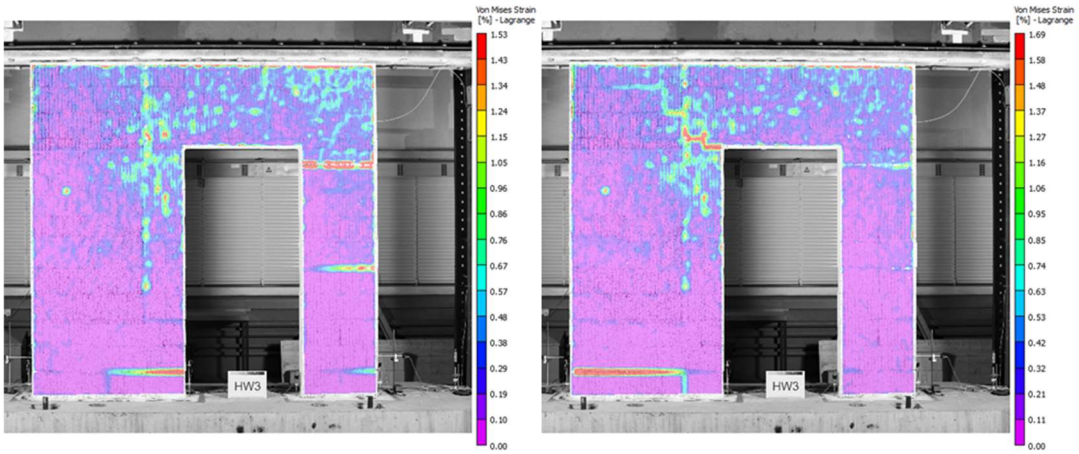

Figure 6: Crack pattern at the target displacement: +5 mm "pulling" (left) and -5mm "pushing" (right) in third load cycle during SLS test

ULS Test

During the ULS test, the wall exhibited a global response similar to the one observed in the SLS test. As expected, opening of the cracks, which were formed during the SLS test, was observed during the loading cycles with target displacements of 3 mm and 6 mm (corresponding to horizontal drift ratios of 0.12% and 0.23%). Further increase of lateral displacements produced additional opening of existing horizontal cracks but the wall continued to show a stable rocking response for lateral displacement applied in pulling direction. Contrarily, for the target displacement of 9 mm (horizontal drift ratio of 0.35%) diagonal shear cracks in the narrower wall segment were formed during the first pushing semi-cycle. Next loading cycles led to further increase of these cracks along the entire wall pier right from the door opening. A drop of approximately 25% of the horizontal force was measured in the corresponding third load cycle. While the wall was pushed to the target displacement of 12 mm (horizontal drift ratio of 0.46%) in the first cycle, rapid decrease of shear strength occured at the horizontal drift ratio of 0.44% resulting in a brittle failure of the wall. Finally, a toe crushing was observed in the wall corner. Crack patterns in the wall mapped by plotting the von Mises strain contours obtained from the DIC analysis for the target displacements of +/- 12 mm (horizontal drift ratio of 0.46%) are shown in Figure 7.

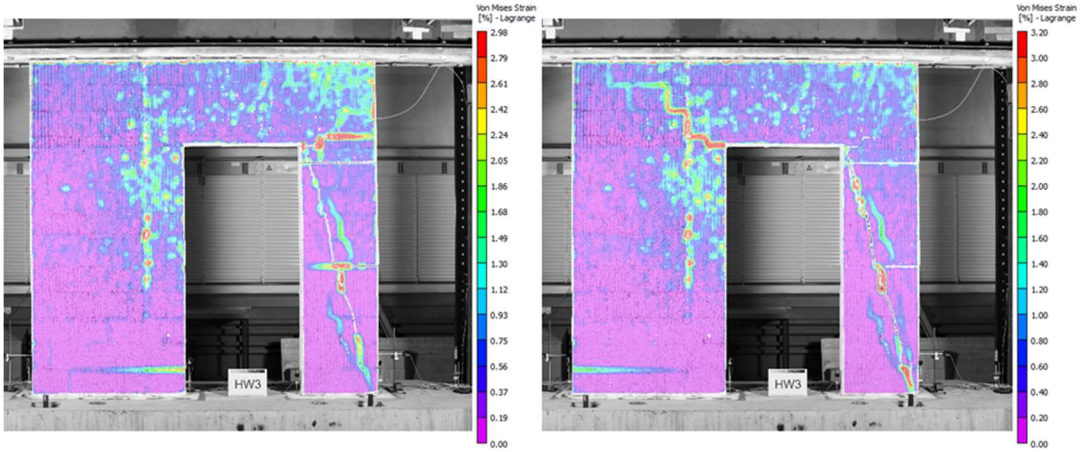

Figure 7: Crack pattern at the target displacement: +12 mm "pulling" (left) and -12mm "pushing" (right) in third load cycle during ULS test

Idealized horizontal force-displacement reponse

From experimentally obtained horizontal force-displacement hysteresis loops for the SLS and the ULS test, the envelope curves for both tests were constructed by connecting the peak horizontal forces of the first loading cycles for each target displacement in the push and the pull directions. Further, they were idealized to bilinear, linear-elastic perfectly plastic, curves assuming equal energy dissipation under envelope curves and idealized horizontal force-displacement curves. The approach proposed in the Swiss Structural Masonry Code recommendations (SIA D0257) [12] was followed. The effective stiffness K_{eff} is determined as the ratio of measured horizontal force $0.7H_{max}$ and its corresponding displacement. The ultimate displacement corresponds to the displacement at which the post peak horizontal force drops by 20% of the maximum horizontal force H_{max}. The ultimate horizontal force H_u is obtained from the equal energy principle. Since the horizontal force-displacement response of the wall was asymmetric, the idealized bilinear responses were determined separately for the push and the pull directions. Generally, the stiffness of the wall in both tests was higher for the pulling than for the pushing load direction. On the other hand, estimated ultimate displacements were larger when the wall was pushed. These differences are more noticeable in the SLS test results due to larger bending moments applied at the wall top. Calculated parameters and idealized bilinear curves of the SLS and the ULS test are given in Table 3 and Figure 8, respectively.

Table 3: Bilinear parameters calculated according to SIA D0257 [6]

Test	Load direction	H_u [kN]	H_u/H_{max}	δ_u [%]	K_{eff} [kN/mm]
SLS	Push	-30.3	0.93	-0.22	42.4
	Pull	43.4	0.92	0.14	54.2
ULS	Push	-38.6	0.95	-0.37	33.8
	Pull	52.2	0.93	0.33	36.7

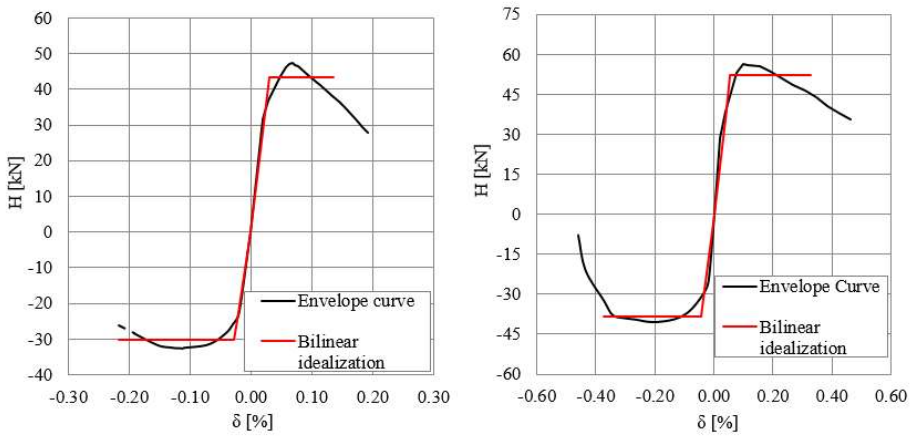

Figure 8: Bilinear idealization of the horizontal load-displacement response: SLS test (left) and ULS test (right)

Stiffness degradation

The formation and propagation of cracks during cyclic lateral loading of URM walls typically lead to stiffness degradation with the increase of applied displacements. The stiffness degradations for the first cycle of each target displacement are shown in Figure 9. At lower drift levels, the effective stiffness of the wall was clearly higher in the pulling direction. However, the effective stiffness in the pulling direction also droped rapidly, resulting in similar effective stiffness in both directions from drift levels of approximately 0.2%. This trend was observed in both tests.

Shear span

In URM buildings floor diaphragms transmit shear forces, affect the shear span of walls and deformed shapes at failure. Thus, the estimation of load-deformation capacity of an URM wall is strongly dependent on the chosen shear span. Typically, these values are determined a priori and assumed independent of lateral displacements. Bending moments at the top and the bottom of the specimen as well as shear spans are determined from the static equilibrium of applied vertical forces and measured force in horizontal actuator. The values of shear spans, determined for the first cycle of applied drift levels in the SLS and the ULS test, are presented in Figure 10. In both tests, from the beginning on, the zero-moment height was located beyond the wall height, i.e. the shear span ratio h_0/h_w was larger than one. With the increase of applied lateral displacement, the height of inflection point in the wall was continuously higher. This trend was more noticeable in the SLS test due to higher bending moments that were applied at wall top in accordance with results from hybrid tests. The jump of shear span ratio for the drift ratio of 0.46% in the push direction was due to damage of the wall and substantial drop of the horizontal force. Therefore, bending of the wall resulted mainly from the bending moment applied at the wall top.

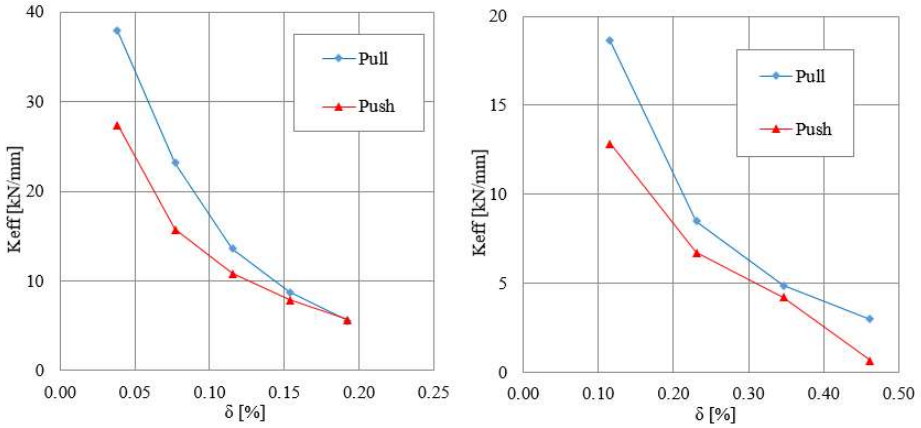

Figure 9: Effective stiffness of the wall for applied lateral displacements: SLS test (left) and ULS test (right)

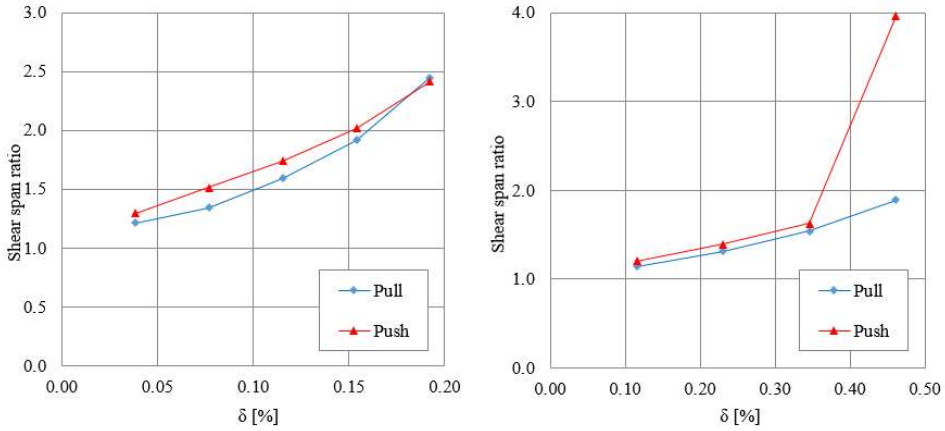

Figure 10: Shear span of the wall for applied lateral displacements : SLS test (left) and ULS test (right)

Comparison of drift capacity with empirical model

The drift capacity of the tested wall was estimated using the empirical model (see Equation 3) proposed by SIA D0257 [12]. SIA D0257 considers the drift capacity as the function of pre-compression level and shear span, independent of the failure mode. The model is limited to the range of shear spans from $(0.5 – 1.0)h_w$. Moreover, it is calibrated based on tests conducted on solid URM walls only.

$$\delta^*_u = 0.7\% \cdot \left(1 - 2.4 \cdot \frac{\sigma_0}{f_x}\right) \cdot \frac{h_0}{h_w} \tag{3}$$

In Table 4, σ_0 and f_x are the pre-compression level and the masonry compressive strength and δ_u are drift capacities resulted from the ULS test. For these drift capacities, shear-span ratios h_0/h_w were obtained (see Figure 10 - right) and further used to estimate drift capacities δ_u^* according to

Equation (3). Empirically calculated ultimate drift capacities are more than twice as high as drift capacities observed in the test. The results showed poor capabilites of the empirical model to predict the drift capacity of an URM wall with asymmetric opening.

Table 4: Estimated drift capacities in the ULS test

Test	Load direction	σ_0 [MPa]	f_x [MPa]	δ_u [%]	h_0/h_w	δ_u^* [%]	δ_u^* / δ_u
ULS	Push	0.64	5.14	0.37	2.11	1.04	2.81
	Pull	0.64	5.14	0.33	1.49	0.73	2.21

SUMMARY AND CONCLUSIONS

The results from two tests on URM wall with an asymmetric door opening were presented and discussed. An eccentric door opening was the reason for the asymmetric force-displacement response. In addition, applied boundary conditions determined in accordance with previous hybrid tests showed significant impact on the results.

Different failure modes were clearly identified for lateral displacements applied in the pull and the push direction. When applying pulling displacements, only horizontal cracks in mortar layers in wall piers on both sides of door opening were created. The effective stiffness was rapidly reduced with the increase of applied lateral displacements. Although the wall showed stable rocking response without signs of potential structural collapse, the obtained drift capacity in the ULS test was only 0.33%. On the other side, increase of applied pushing displacements caused significant increase of normal stresses and formation of diagonal shear cracks in the narrower wall pier. For target displacement of 12 mm, the wall experienced a brittle shear failure and the estimated drift capacity was 0.37%.

The comparison between experimentally obtained drift capacities with drift capacities determined using empirical model proposed in Swiss Structural Masonry Code showed poor agreement in results. The empirically obtained drift capacities significantly overestimated the actual determined drift capacity in the experiment. The work presented here shows that direct application of the empirical model on perforated URM walls can lead to unrealistic results.

Additional research is necessary in following directions. First, more hybrid tests are needed to simulate and understand the response of such walls to earthquake ground motions. Further, such tests should support better definition of boundary conditions and loading histories for quasi-static cyclic tests. Second, further development of the empirical models that can account for broader range of geometrical properties and boundary conditions is necessary.

ACKNOWLEDGEMENTS

We wish to acknowledge Mr. Dominik Werne, Mr. Pius Herzog and Mr. Thomas Jaggi from the Laboratory of Structural Engineering of ETH Zürich for supporting the realization of experiments.

REFERENCES

[1] Ingham, J. M. and Griffith, M. C. (2011). "The performance of unreinforced masonry buildings in the 2010/2011 Canterbury earthquake swarm." Christchurch, Canterbury Earthquakes Royal Commission of Inquiry.

[2] Beyer, K. and Dazio, A. (2012). "Quasi-static cyclic tests on masonry spandrels." *Earthquake Spectra*, 28(3), 907-929.

[3] Allen, C., Masia, M.J., Page, A.W., Griffith, M.C., Derakhshan, H. and Mojsilovic, N. (2016). "Experimental testing of unreinforcem masonry walls with openings subject to cyclic in-plane shear" *Proceedings, 16th International Brick/Block Masonry Conference*, Padova, Italy, 1401-1408.

[4] Knox, C. L., Dizhur, D. and Ingham, J. M. (2016). "Experimental cyclic testing of URM pier-spandrel substructures" *J. Struct. Eng.,* 143 (2): 04016177.

[5] Triller, P., Tomaževič, M. and Gams, M. (2016). "Seismic behaviour of multistorey plain masonry shear walls with openings: An experimental study" *Proceedings, 16th International Brick/Block Masonry Conference*, Padova, Italy, 1949-1955.

[6] Howlader, M. K., Masia, M.J. and Griffith, M. C. (2020). "In-Plane Response of Perforated Unreinforced Masonry Walls under Cyclic Loading: Experimental Study", *J. Struct. Eng.,* 146(6): 04020106.

[7] EN 772–1:2011 (2011). Methods of test for masonry units, Part 1: Determination of compressive strength. European Committee for Standardization (CEN), Brussels.

[8] EN 1015–11:1999. (1999) Methods of test for mortar for masonry, Part 11: Determination of flexural and compressive strength of hardened mortar. European Committee for Standardization (CEN), Brussels.

[9] EN 1052–1:1998 (1998). Methods of test for masonry, Part 1: Determination of compressive strength. European Committee for Standardization (CEN), Brussels.

[10] Miraglia, G., Petrović, M., Abbiati, G., Mojsilović, N. and Stojadinović, B. (2020). "A Model-Order Reduction Framework for Hybrid Simulation based on Component-Mode Synthesis" *Earthquake Engineering and Structural Dynamics*, 49(8), 737-753.

[11] Mojsilović, N. and Salmanpour, A.H. (2016). "Masonry walls subjected to in-plane cyclic loading: Application of Digital Image Correlation for deformation field measurement", *International Journal of Masonry Research and Innovation,* 1(2), 165-187.

[12] SIA D 0257 (2015). "*Bemessungsbeispiele zur Norm SIA 266"*, Schweizerischer Ingenieur- und Architektverein, Zürich.